

ORIGINAL ARTICLE

Metabolic and physiological interdependencies in the *Bathymodiolus azoricus* symbiosis

Ruby Ponnudurai^{1,8}, Manuel Kleiner^{2,8}, Lizbeth Sayavedra³, Jillian M Petersen^{3,4}, Martin Moche⁵, Andreas Otto⁵, Dörte Becher⁵, Takeshi Takeuchi⁶, Noriyuki Satoh⁶, Nicole Dubilier³, Thomas Schweder^{1,7} and Stephanie Markert^{1,7}

¹Institute of Pharmacy, Ernst-Moritz-Arndt-University, Greifswald, Germany; ²Department of Geoscience, University of Calgary, Calgary, Canada; ³Department of Symbiosis, Max Planck Institute for Marine Microbiology, Bremen, Germany; ⁴Division of Microbial Ecology, University of Vienna, Vienna, Austria; ⁵Institute of Microbiology, Ernst-Moritz-Arndt-University, Greifswald, Germany; ⁶Marine Genomics Unit, Okinawa Institute of Science and Technology, Okinawa, Japan and ⁷Institute of Marine Biotechnology, Greifswald, Germany

The hydrothermal vent mussel *Bathymodiolus azoricus* lives in an intimate symbiosis with two types of chemosynthetic Gammaproteobacteria in its gills: a sulfur oxidizer and a methane oxidizer. Despite numerous investigations over the last decades, the degree of interdependence between the three symbiotic partners, their individual metabolic contributions, as well as the mechanism of carbon transfer from the symbionts to the host are poorly understood. We used a combination of proteomics and genomics to investigate the physiology and metabolism of the individual symbiotic partners. Our study revealed that key metabolic functions are most likely accomplished jointly by *B. azoricus* and its symbionts: (1) CO₂ is pre-concentrated by the host for carbon fixation by the sulfur-oxidizing symbiont, and (2) the host replenishes essential biosynthetic TCA cycle intermediates for the sulfur-oxidizing symbiont. In return (3), the sulfur oxidizer may compensate for the host's putative deficiency in amino acid and cofactor biosynthesis. We also identified numerous 'symbiosis-specific' host proteins by comparing symbiont-containing and symbiont-free host tissues and symbiont fractions. These proteins included a large complement of host digestive enzymes in the gill that are likely involved in symbiont digestion and carbon transfer from the symbionts to the host.

The ISME Journal (2017) 11, 463–477; doi:10.1038/ismej.2016.124; published online 1 November 2016

Introduction

Life at deep-sea hydrothermal vents is powered by chemosynthetic bacteria, many of which live in symbiosis with animals. Hydrothermal vents of the Mid-Atlantic Ridge (MAR) are home to the mytilid bivalve *Bathymodiolus azoricus*, which harbours two types of gammaproteobacterial endosymbionts (von Cosel *et al.*, 1999; Van Dover, 2000; Duperron *et al.*, 2006). Unlike other vent symbioses, such as the giant tube worm *Riftia pachyptila* and the clam *Calyptogena* spp., which display extreme dependence on their chemoautotrophic endosymbionts for nourishment (Childress and Fisher, 1992), *B. azoricus* are mixotrophs: They possess a functional gut and feeding groove for filter feeding in addition to the chemosynthetic symbionts in their

gills (Page *et al.*, 1991; Gustafson *et al.*, 1998; von Cosel *et al.*, 1999; Riou *et al.*, 2010). Filter-feeding may supplement the symbiotic diet of the host with particulate and organic matter from their surroundings (Le Pennec *et al.*, 1990) and may also enable them to survive without symbionts for limited periods of time (Colaco *et al.*, 2011). However, aposymbiotic *B. azoricus* in laboratory aquaria display an overall reduction in their fitness and health (Raulfs *et al.*, 2004; Kádár *et al.*, 2005), suggesting that despite their nutritional flexibility, *B. azoricus* mussels depend on their symbionts for long-term sustenance.

B. azoricus maintains a stable symbiotic partnership with two distinct gammaproteobacterial phylotypes living within its gills (Figure 1). The co-occurrence of a thiotrophic symbiont, which oxidizes reduced sulfur compounds, and a methanotroph, which oxidizes methane (Fiala-Médioni *et al.*, 2002), enables *B. azoricus* to simultaneously tap the energy from two of the most abundant reductants in the MAR vent fluids. The symbionts are housed in vacuoles within specialized gill epithelial cells called bacteriocytes. The

Correspondence: S Markert, Pharmaceutical Biotechnology, Institute of Marine Biotechnology, Walther-Rathenau-Straße 49A, Greifswald, 17489 Germany.

E-mail: stephanie.markert@uni-greifswald.de

⁸These two authors contributed equally to this work.

Received 14 June 2016; revised 28 July 2016; accepted 10 August 2016; published online 1 November 2016

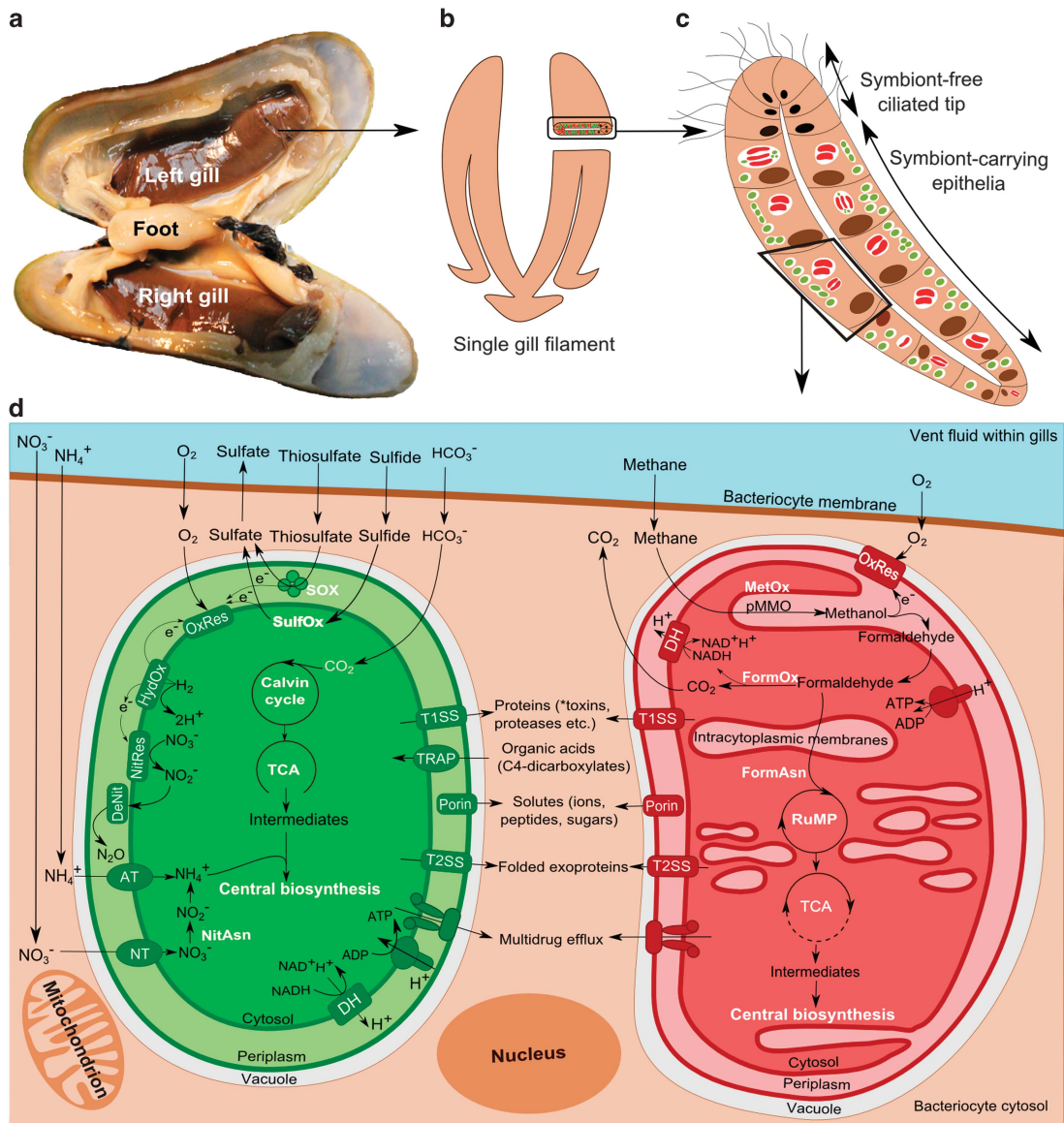


Figure 1 Schema of a *B. azoricus* gill bacteriocyte. (a) Dissected *B. azoricus* specimen showing gills and gill filaments. (b) Schema of single gill filament. (c) Schematic cross-section of a gill filament showing bacteriocytes. (d) A single bacteriocyte showing the central pathways of the symbionts. Symbionts (thiotroph: green, methanotroph: red) are located inside vacuoles (white) surrounded by the bacteriocyte cytosol (brown) with gases and substrates exchanged between vent fluids (blue) flushing the gills. An overview of the basic metabolic processes occurring in the symbionts is shown. AT: ammonium transporter, DH: dehydrogenase, DeNit: denitrification, FormAsn: formaldehyde assimilation, FormOx: formaldehyde oxidation to formate and CO₂, HydOx: hydrogen oxidation, MetOx: methane oxidation by pMMO (particulate methane-monoxygenase enzyme complex) to methanol and then to formaldehyde (see Supplementary Figure S2B for details), NitAsn: nitrogen assimilation, NitRes: nitrate respiration (see Supplementary Figure S4 for details on nitrogen metabolism), NT: nitrate transporter, OxRes: Oxidative phosphorylation with oxygen as terminal electron acceptor, SOX: thiosulfate oxidation, SulfOx: sulfide oxidation via the rDSR-APS-Sat pathway (see Supplementary Figure S2A), TCA: tricarboxylic acid cycle, TRAP: tripartite ATP-independent periplasmic transporter, T1SS: Type I secretion system, T2SS: Type II secretion system. *toxins are known to be secreted by the thiotrophs (Sayavedra *et al.*, 2015).

bacteriocytes face the apical side of the gill filament, which is in contact with the vent fluids (Figure 1; Distel *et al.*, 1995). The physical proximity of the bacteriocytes to the ambient vent fluids facilitates direct exchange of dissolved gases and substrates (Childress and Fisher, 1992) and may also allow quick responses of symbionts to changes in environmental conditions. The host

presumably acquires nutrients from the symbionts by digesting them using lysosomal degradation enzymes (Streams *et al.*, 1997; Fiala-Médioni *et al.*, 2002; Kádár *et al.*, 2008).

The symbionts' location within host bacteriocytes allows for intricate metabolic interactions between the host and the symbionts. So far, only a handful of whole gill-based 'omics' studies have examined this

complex association, most of them focusing on the physiology of the host (Bettencourt *et al.*, 2010; Company *et al.*, 2011; Petersen *et al.*, 2011; Sayavedra *et al.*, 2015). The fact that the symbionts are uncultivable as yet and the mussels can only be maintained temporarily under controlled laboratory conditions (Kádár *et al.*, 2005) has rendered detailed physiological investigations difficult. We therefore conducted a culture-independent proteogenomic study, which – for the first time – provided a detailed and comprehensive picture of host–symbiont interaction dynamics and metabolic interdependencies in *B. azoricus*. To detect host proteins potentially involved in symbiosis-specific functions, we compared protein expression patterns between symbiont-containing and symbiont-free host tissues.

Experimental procedures

Sampling of Bathymodiolus mussels and differential enrichment for proteomics

Sampling details and biological replicate numbers for all analyses performed in this study are summarized in Supplementary Table S1A. For proteome analyses, *B. azoricus* mussels were collected from the Menez Gwen vent field on the MAR at 37°50'41" N, 31°31'10" W during the RV Meteor cruise M82-3 as described by Sayavedra and colleagues (2015). The mussels were dissected, gill tissue was removed and homogenized in 1x PBS (Figure 2, see Supplementary Methods for a detailed description of the enrichment procedure). The homogenate was subjected to a combination of differential pelleting and rate-zonal centrifugation using density gradients on board the research vessel to separate the symbionts and host components from each other (Figure 2). The composition of putative host- and symbiont-enriched fractions after centrifugation was analysed using catalyzed reporter deposition-fluorescence *in situ* hybridization (CARD-FISH, see Supplementary Information). Based on the CARD-FISH evaluation, the host-enriched supernatant (containing soluble host proteins) and the symbiont-enriched gradient pellet (containing both symbionts, but particularly enriched in the thiotroph) were chosen for further proteomic analysis (Figure 2). Additionally, complete gill and foot tissue samples from the same animals that were processed by centrifugation were also frozen at –80 °C to enable comparisons between the proteomes of whole tissues and of host- and symbiont-enriched fractions.

Proteomic analysis

Specific details of the protein extraction procedure, 1D-PAGE, LC-MS/MS, protein identification, validation and quantitation can be found in the Supplementary Methods section. Briefly, soluble proteins and membrane-associated proteins were extracted from enriched gradient fractions in

biological triplicates (that is, from three *B. azoricus* individuals) and from whole tissue samples in biological duplicates (for replicate numbers of all MS measurements see Supplementary Table S1B). Proteins were separated using 1D-PAGE and in-gel digested with trypsin. Resulting peptides were separated by liquid chromatography and analysed simultaneously by coupling the liquid chromatography online to a mass spectrometer. For identification of host and symbiont proteins, all MS/MS spectra were searched against a comprehensive protein database (see Supplementary Methods and Supplementary Table S2A for a list of all organisms whose protein sequences are included in the database). For relative semi-quantitative analysis of proteins, normalized spectral abundance factor (NSAF) values were calculated for each sample (NSAF%, Florens *et al.*, 2006). NSAFs were subsequently also normalized for each organism individually (OrgNSAF%, Mueller *et al.*, 2010).

Statistical analyses for the identification of putative symbiosis-relevant proteins

To identify potentially symbiosis-relevant host and symbiont proteins we did a statistical comparison of protein abundances in different sample types. For host proteins that may play a direct role in the symbiosis we tested for proteins whose NSAF values differ significantly between the symbiont-containing gill samples (whole gill and gill supernatant) versus the symbiont-free foot tissue. Host proteins that are potentially involved in direct interactions with the symbionts (that is, physically linked to the symbionts) were 'pulled down' by the symbionts during centrifugation-based symbiont enrichment. We identified these proteins by testing for host protein abundances that were significantly higher in the symbiont-enriched gradient pellet versus the whole gill samples and the gill supernatant. Statistical evaluation of differences between samples involved Log transformations of NSAF%/OrgNSAF% values followed by *t*-test, all of which were done using the Perseus software (version 1.4.1.3, <http://www.perseus-framework.org/doku.php>) as described in the Supplementary Methods.

Data accessibility

The mass spectrometry proteomics data and the protein sequence database were uploaded to the ProteomeXchange Consortium via the PRIDE (Vizcaino *et al.*, 2016) partner repository with the dataset identifier PXD004061 (DOI: 10.6019/PXD004061). Nucleotide and protein sequence information for the methanotrophic symbionts of *B. azoricus* and of *Bathymodiolus* sp. was deposited in GenBank under the BioProject accession numbers PRJEB13769 and PRJEB13047, respectively.

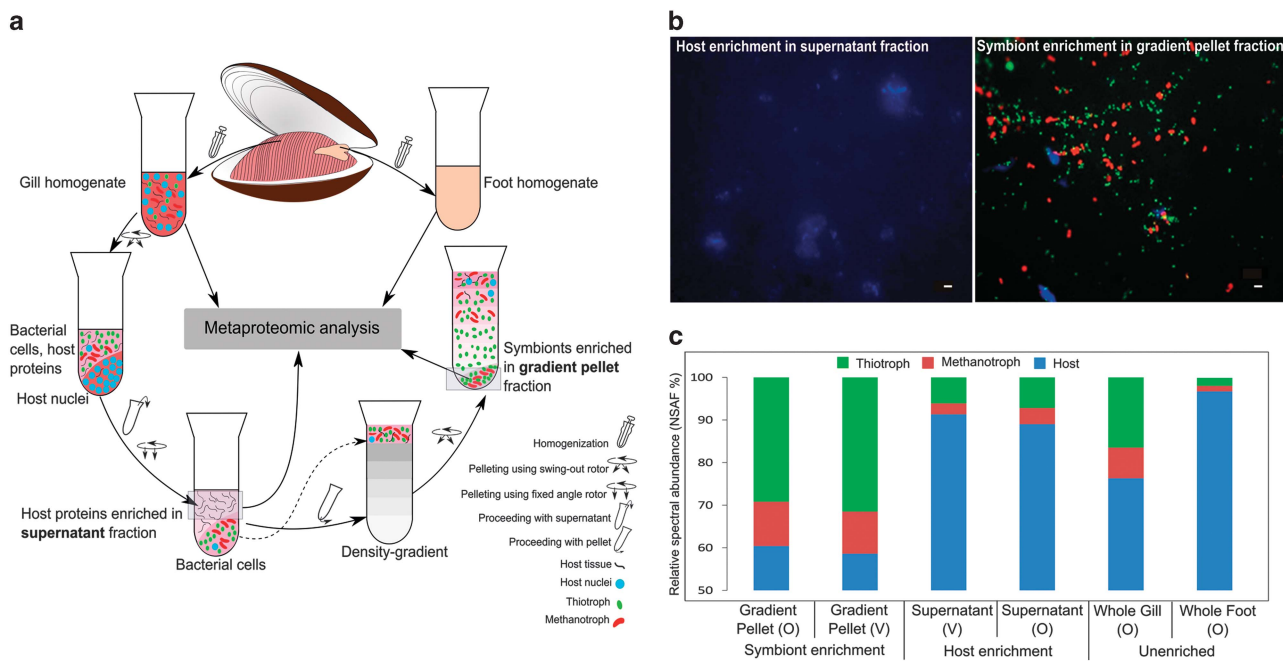


Figure 2 Density gradient enrichment of symbiont cells and host components followed by CARD-FISH. (a) Step-wise workflow of the density gradient enrichment method for physical separation of *B. azoricus* host and symbiont cells. Sampling for tissue-based metaproteomic analysis of whole gill and foot tissue is also shown. Bold font: enriched fractions elaborated in panel b and c. (b) Epifluorescence micrographs of supernatant (left) and gradient pellet (right) fractions obtained from the enrichment method shown in panel a. Green CARD-FISH signal: thiotrophs; red CARD-FISH signal: methanotrophs; blue DAPI signal: host. Scale bar: 2 μ m. (c) Enhanced spectral abundance of symbiont- and host-associated proteins in density gradient-based enrichments (symbiont-enriched gradient pellet and host-enriched supernatant) as compared to unenriched (gill and foot) tissues. Stacked bars show the % of spectral abundance (calculated by summing up NSAF% and averaging it across biological replicates) contributed by thiotrophs, methanotrophs and host, respectively, to the total spectral abundance of each sample type. O: proteins identified by LTQ-Orbitrap Classic MS/MS analysis ($n = 3$), V: proteins identified by LTQ-Orbitrap Velos MS/MS analysis ($n = 2$, see Methods).

Results and discussion

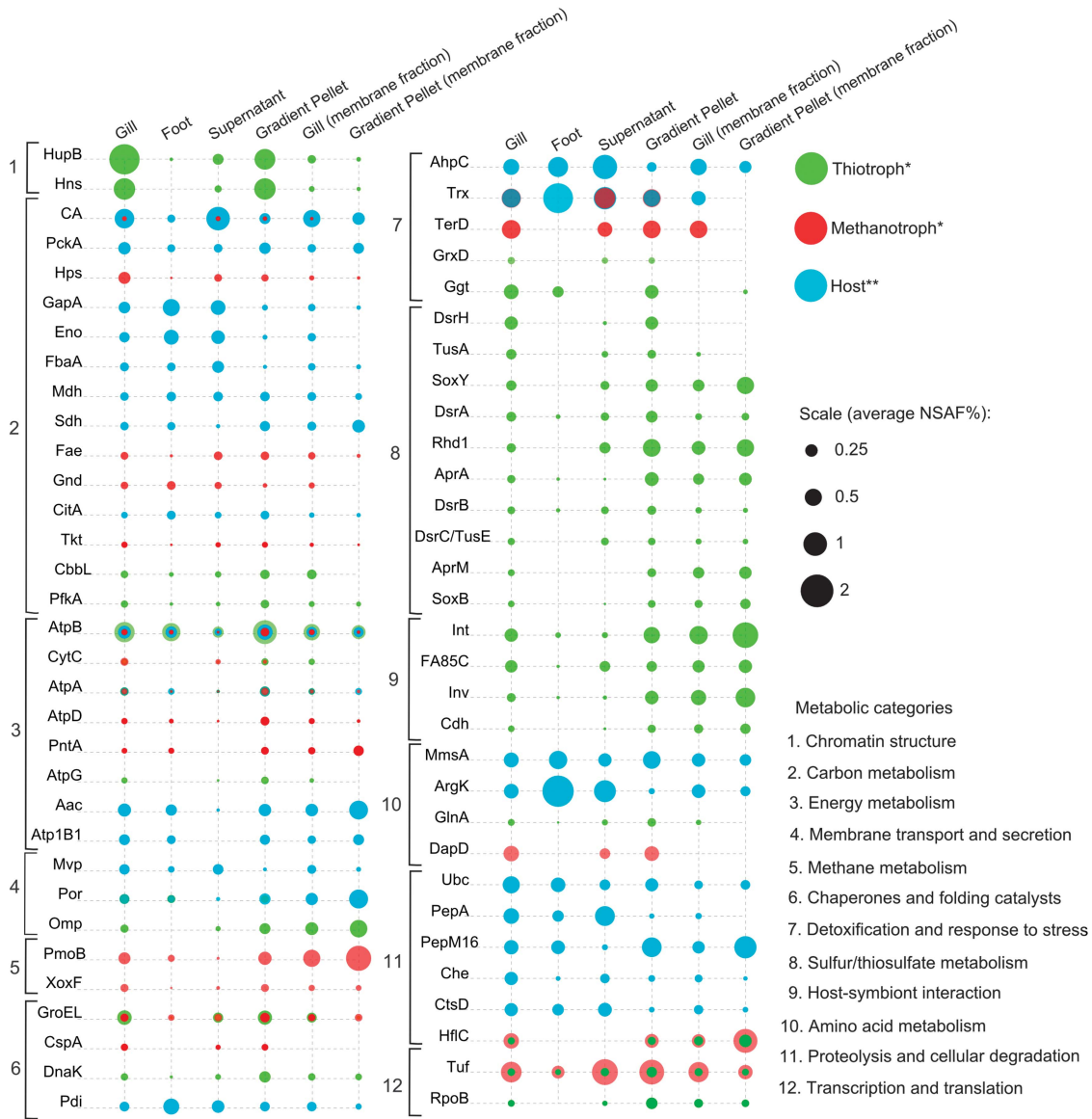
Enhanced protein identification following density gradient enrichment in *B. azoricus*

We used a multistep centrifugation technique to physically separate host components and thiotrophic and methanotrophic symbiont cells of *B. azoricus*. This enrichment substantially enhanced the rate of spectral identifications for the respective individual organisms, as compared to plain, unenriched tissue. Our centrifugation procedure involved differential pelleting of host nuclei followed by rate-zonal density gradient centrifugation for symbiont enrichment (Figure 2a). We analysed the resulting fractions with CARD-FISH and DAPI staining to identify fractions where either host material or symbiont cells were enriched (Figure 2b). Relative cell counts revealed that 93% of the cells in the gradient pellet were thiotrophic and methanotrophic endosymbionts and that 97% of the solid material in the supernatant consisted of host nuclei and host cell fragments (see Supplementary Figure S1). This enrichment was clearly reflected in our proteomic results, where we found a 17.7% increase in symbiont-associated spectral identifications (NSAF) in the symbiont-enriched gradient pellet, and a 15% increase in host spectral identifications in the host-enriched supernatant, as compared to the gill tissue

(Figure 2c). The enhanced spectral identification rate enabled better quantification of the identified proteins and substantially improved the proteome coverage: The number of identified proteins in enriched samples increased by 7.4% (host proteins) and 9.3% (symbiont proteins) compared to those from unenriched tissues (Supplementary Table S2C, see Supplementary Results and Discussion for absolute numbers of identified proteins). Grouping of the most abundant proteins (in terms of NSAF%) of the symbiotic partners into metabolic categories allowed us to trace the metabolic network of the *B. azoricus* consortium (Figure 3).

The B. azoricus symbiosis is fuelled by a versatile array of energy sources

Thiosulfate oxidation. In the thiotrophic *B. azoricus* symbiont, thiosulfate as an energy source seems to play a more prominent role than in other chemoautotrophic symbioses. We found the thiotroph's SoxYZ proteins for thiosulfate oxidation (Sox) to be more abundant than the dissimilatory sulfite reductase (Dsr) enzymes DsrAB for hydrogen sulfide oxidation: With 1.104 OrgNSAF% (SoxYZ) and 0.894 OrgNSAF% (DsrAB), the enzyme complexes were present in a DsrAB:SoxYZ ratio



of 0.81 (soluble protein fraction of gradient pellet samples, Velos analysis, see Supplementary Table S3). In contrast, the sulfur-oxidizing symbionts of *R. pachyptila* and *Olavius algarvensis* express DsrAB at much higher levels than SoxYZ. The DsrAB:SoxYZ ratio in the *Riftia* symbiont was 2.5 ($n=3$; S. Markert, unpublished results), and 5.2 in the *Olavius* Gamma 1 symbiont (Kleiner *et al.*, 2012b). In addition to the Sox enzyme complex, we identified two sulfur/thiosulfate carrier protein homologs, a TusA domain-containing protein (Rhd1,

BazSymB_scaffold00007_23) and a Rhodanese-like domain-containing protein (Rhd2, BazSymB_scaffold00002_24) in the *B. azoricus* thiotroph (Supplementary Figure S2A). In fact, Rhd1 was one of the most abundant proteins in the thiotroph's membrane proteome (membrane OrgNSAF% from gradient pellet, Supplementary Table S3). Rhodanese cleave thiosulfate to sulfite and sulfide (Brune, 1995, Supplementary Figure S2A), while TusA has been shown to mediate thiosulfate transfer in an acidothermophilic sulfur- and tetrathionate-oxidizing

archaeon (Liu *et al.*, 2014). Both rhodanese proteins together constituted 2.11 OrgNSAF% in the thiotrophic *B. azoricus* symbiont (for comparison: the *Riftia* symbiont's rhodanese proteins make up only 0.15 OrgNSAF %, $n=3$; S. Markert, unpublished). The *B. azoricus* thiotroph clearly oxidizes sulfide, as indicated by the detection of most components of the rDSR-APS-Sat pathway (see Supplementary Results and Discussion). However, the relatively high expression of thiosulfate-metabolizing and -transfer enzymes (compared to the sulfur-oxidizing symbionts of other host animals) indicates that thiosulfate oxidation may be particularly important for the *B. azoricus* symbiosis in its specific habitat. This is in agreement with previous studies, in which thiosulfate was observed to stimulate carbon fixation much more than sulfide in the thiotrophic symbionts of related *Bathymodiolus* species (Belkin *et al.*, 1986; Fisher *et al.*, 1987).

Thiosulfate is more stable than sulfide and is less toxic to aerobic respiration (Harada *et al.*, 2009). In other symbiotic species such as vestimentiferan tubeworms and vesicomyid clams, sulfide is transported in a less harmful form, bound to the host's hemoglobin (Arp *et al.*, 1984, 1987; Doeller *et al.*, 1988). However, no dedicated host proteins for sulfide transport are known in *Bathymodiolus* mussels (Powell and Somero, 1986). High concentrations of thiosulfate (0.178 mM in gills versus 0.079 mM in other tissues) in the closely related *B. thermophilus* led Fisher *et al.* (1988) to propose that the host may detoxify sulfide from the environment to the less toxic thiosulfate. Host-mediated thiosulfate production as a means of sulfide detoxification was recently also suggested for *B. brevior* (Beinart *et al.*, 2015). If *B. azoricus* uses a similar mechanism of sulfide detoxification, then its symbionts would be exposed to thiosulfate concentrations that are much higher than those in the environment. This may stimulate higher expression of thiosulfate-metabolizing enzymes in the *B. azoricus* thiotroph as compared to other symbionts, whose hosts do not produce thiosulfate as a means of sulfide detoxification.

Hydrogen oxidation. In addition to its capacity for thiotrophy, the *B. azoricus* thiotroph is also capable of using hydrogen (H_2) as an electron acceptor (Petersen *et al.*, 2011). Genes for hydrogen oxidation were clearly expressed, but at lower abundance compared with enzymes involved in sulfide or thiosulfate oxidation. H_2 oxidation may therefore not be as important as the oxidation of reduced sulfur compounds for the thiotroph under the conditions prevailing at the sampling site in this study (see Supplementary Figure S2A and Supplementary Results and Discussion).

Methane oxidation. The energy-generating methane oxidation process is the most prominent metabolic pathway in the methanotrophic *B. azoricus* symbiont.

Its key enzymes, the particulate methane monooxygenase PmoCAB and the methanol dehydrogenase XoxF that catalyze the oxidation of methane to formaldehyde, constituted 28.6% of the membrane OrgNSAF in the gradient pellet samples and 2.4% of the gill OrgNSAF, respectively (Supplementary Figure S2B, Supplementary Results and Discussion). Considering the high catalytic efficiency of both enzymes (Chan *et al.*, 2013; Keltjens *et al.*, 2014), these high expression levels likely correspond to very high methane oxidation rates in the *B. azoricus* methanotroph. As indicated by our results, the symbiont can accomplish the subsequent energy-producing oxidation of formaldehyde to formate and CO_2 via two parallel metabolic routes, that is, the tetrahydrofolate (H_4F) pathway and the dephosphotetrahydromethanopterin (H_4MPT) pathway (see Supplementary Figure S3 and Supplementary Results and Discussion for details). We identified enzymes of both pathways in the methanotroph's proteome. The presence of multiple routes for formaldehyde metabolism may offer enhanced metabolic flexibility to the symbiont under various environmental conditions. Also, since accumulation of formaldehyde is toxic to the cells, the two formaldehyde oxidation pathways may operate as overflow valves for controlling excess formaldehyde levels, while simultaneously generating electrons and reducing equivalents during the process (Crowther *et al.*, 2008).

Pathways for carbon assimilation are highly expressed in both symbionts while crucial TCA cycle enzymes are missing in the thiotroph

Assimilation of C1 compounds. In the proteomes of both the thiotrophic and the methanotrophic *B. azoricus* symbiont, carbon fixation pathways were highly abundant, reflecting their importance in the symbiotic association. The thiotroph uses the Calvin-Benson-Bassham cycle for autotrophic fixation of CO_2 (see Supplementary Results and Discussion and Figure 4a). All Calvin-Benson-Bassham pathway enzymes were highly abundant in the thiotroph. The large subunit of ribulose biphosphate carboxylase/oxygenase (RuBisCO form I, CbbL, BazSymA_Acontig00018_18), the key enzyme of the Calvin-Benson-Bassham cycle, was consistently the most abundant enzyme of the thiotroph's carbon metabolism in all samples analysed in our study (Figures 3 and 4a, Supplementary Table S3). The methanotroph expressed a complete ribulose monophosphate (RuMP) pathway for the assimilation of carbon from formaldehyde, as well as parts of a second carbon assimilation pathway, the serine cycle (see Figure 4b, Supplementary Figure S3 and Supplementary Results and Discussion). The high abundance of the two RuMP pathway key enzymes hexulose-6-phosphate formaldehyde lyase (Hps, BAZMOX_41472_2) and 3-hexulose-6-phosphate isomerase (Hpi1, BAGiLS_016202) indicates that the methanotroph primarily uses this pathway for

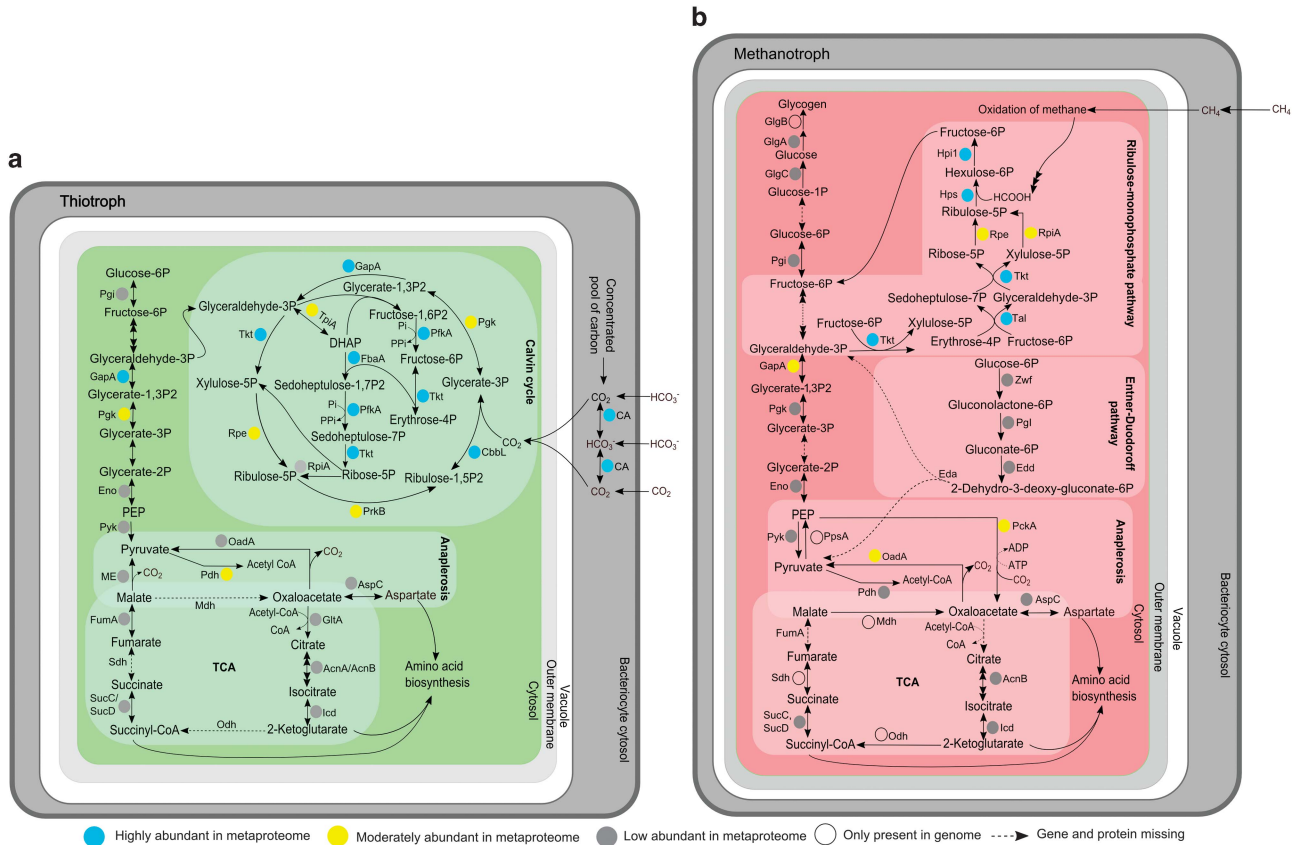


Figure 4 Central carbon metabolism in *B. azoricus* symbionts. **(a)** In the thiotrophic symbiont. **(b)** In the methanotrophic symbiont. Eda: KHG/KDPG aldolase, GlgB: 1,4- α -glucan branching enzyme, Mdh: Malate dehydrogenase, ME: malic enzyme, Odh: 2-oxoglutarate dehydrogenase, PpsA: PEP synthase, Sdh: succinate dehydrogenase. For functions of enzymes that were detected as proteins in this study refer to Supplementary Table S3. Protein abundances correspond to average OrgNSAF% in the respective organism from whole gill tissue samples (in Velos MS/MS measurements, see Supplementary Table S2B for genome assemblies used for gene prediction. Multiple arrows indicate multiple enzymatic steps. Dotted arrows indicate enzymes that are missing in the respective symbiont's genome. Sizes are not drawn to scale.

formaldehyde assimilation. The serine cycle seems to play a minor role in carbon assimilation as compared to the dominant RuMP pathway under the conditions in this study (see Supplementary Results and Discussion).

Incomplete TCA cycle in the thiotroph. The thiotrophic symbiont of *B. azoricus* appears to be unable to replenish the crucial carbon metabolism intermediates oxaloacetate and succinate. As expected in an obligate autotroph, the thiotroph lacks the tricarboxylic acid (TCA) cycle enzyme 2-oxoglutarate dehydrogenase (Odh; Wood *et al.*, 2004; Kleiner *et al.*, 2012a). The absence of Odh effectively prevents wasteful re-oxidation of autotrophically fixed organic carbon, while still allowing for the production of carbon precursors for amino acid biosynthesis and other anabolic pathways. Intermediates of this 'horse shoe' TCA cycle are usually replenished by anaplerotic pathways such as the glyoxylate bypass. Surprisingly, our proteogenomic analysis revealed that not only the gene encoding Odh is missing in the thiotroph, but also the genes for the TCA cycle enzymes malate dehydrogenase (Mdh) and succinate dehydrogenase (Sdh,

Figure 4a). Moreover, the thiotroph apparently lacks all known genes encoding anaplerotic enzymes for the replenishment of the essential TCA cycle intermediates oxaloacetate and succinate (see Supplementary Results and Discussion), although it expresses enzymes involved in oxaloacetate and succinate consumption (Figure 4a). Oxaloacetate is an important precursor for biosynthesis of essential amino acids of the aspartate family, while succinate, or rather its derivative succinyl-CoA, is required for the biosynthesis of porphyrins and amino acids. Replenishment of oxaloacetate and succinate is therefore crucial for cellular metabolism and alternate mechanisms for refilling both intermediates must exist (see below).

Complete TCA cycle in the methanotroph. Unlike the thiotrophic symbiont of *B. azoricus*, the methanotroph has a complete set of genes encoding TCA cycle enzymes, including *odh* (BAZMOX_25028_0). Odh, Mdh and Sdh were, however, not detected in the methanotroph's proteome (Figure 4b). In the facultative methylotroph *Methylobacterium extorquens* AM1, *odh* expression is repressed during growth on C1-compounds (Chistoserdova *et al.*, 2003). It is therefore

possible that the methanotrophic symbiont of *B. azoricus* expresses a complete, energy-producing TCA cycle during growth on multicarbon compounds when the preferred carbon source methane is not available, and an incomplete version of the TCA cycle that produces anabolic intermediates when methane is plentiful (Zhao and Hanson, 1984; Chistoserdova *et al.*, 2003; Wood *et al.*, 2004; Dedysh *et al.*, 2005). In the absence of methane, cellular storage polymers such as glycogen may serve as readily available multicarbon compounds for energy generation. This idea is supported by the detection of glycogen synthesis enzymes in the methanotroph's proteome (Figure 4b, Supplementary Table S3, Supplementary Results and Discussion).

Some metabolic tasks are accomplished jointly by the symbiotic partners

CO₂ concentration by carbonic anhydrase in gills. In the *B. azoricus* gill metaproteome, host-derived carbonic anhydrase (CA) is one of the most abundant proteins expressed (Figures 3 and 4a, Supplementary Table S3, BAGiLS_000922). The enzyme was ~10 times more abundant in gills and ~19 times more abundant in the supernatant, respectively, as compared to symbiont-free foot tissue (Table 1), suggesting a symbiosis-specific role for the host CA in *B. azoricus*. In marine invertebrates such as anemones, corals, tubeworms and clams harbouring carbon-fixing bacteria, the ubiquitous enzyme CA facilitates the reversible conversion of bicarbonate, the dominant form of seawater carbon, to CO₂ for transport to symbiont-bearing tissues (Kochevar and Childress, 1996). The *B. azoricus* CA therefore likely represents a CO₂-concentrating mechanism, which provides elevated levels of inorganic carbon for fixation by the thiotrophic symbiont (Figure 4a). High activity and protein expression of host CA was also described in gills of *Bathymodiolus* mussels hosting only methanotrophic symbionts, where CA may be involved in the elimination of CO₂ produced as an end product of methane oxidation (Hongo *et al.*, 2013). In addition to the host CA, we also found the CAs of the thiotroph and of the methanotroph expressed (BAT01672, BAZMOX_02303_3), albeit in very low abundances. It is unclear whether either of the CAs from host, methanotroph or thiotroph participate in the elimination of methanotroph-derived CO₂. We speculate that in *B. azoricus* this methanotroph-derived CO₂, instead of being eliminated, may be recycled by the thiotrophic symbiont for CO₂ fixation (Nelson and Fisher, 1995).

Biosynthesis of amino acids and vitamins/cofactors in B. azoricus. Only seven genes associated with amino acid biosynthesis were found in the *B. azoricus* host EST library, of which four were identified as proteins (Supplementary Figure S5). In contrast, the genome of the thiotrophic symbiont

contains essentially complete gene sets for the biosynthesis of all 20 proteinogenic amino acids and of 11 vitamins and cofactors. Ninety-five per cent of the thiotroph's amino acid synthesis-related genes (that is, 63 of 66) and 43% (26 out of 60) of the genes associated to cofactor biosynthesis were identified as proteins (Supplementary Figure S5). In the methanotroph, 43 amino acid synthesis genes and 30 cofactor synthesis genes were detected in the genome, of which 30 (70%) and 11 (37%), respectively, were detected at the protein level (Supplementary Figure S5). As amino acids are indispensable for protein biosynthesis in the host, the sparse presence of amino acid synthesis-related genes in *B. azoricus* (even when considering the incompleteness of the available transcriptome information) may indicate that the bivalve depends on its symbionts for supply with amino acids and cofactors. This putative deficiency in amino acid biosynthetic enzymes seems to be uncommon in non-symbiotic marine mussels as several species are capable of *de novo* synthesizing most amino acids from TCA pathway intermediates (Ellis *et al.*, 1985). *Bathymodiolus* mussels can acquire amino acids by direct uptake from seawater or from breakdown of organic matter ingested through filter feeding (Riou *et al.*, 2010). But whether this can satisfy all of their nutritional requirements is unclear (Martins *et al.*, 2008), particularly given the unsteady availability of organic nutrients in the dynamic vent habitats. Our results suggest that the *B. azoricus* symbionts are capable of providing their host with all required amino acids and prosthetic groups, a scenario that was previously also suggested for the thiotrophic vesicomycid symbioses of *Calyptogena magnifica* and *C. okutanii* (Newton *et al.*, 2008). Amino acids that are synthesized by the *B. azoricus* symbionts may be made available to the host through intracellular symbiont digestion, as indicated by the detection of abundant host-derived digestive enzymes in the gill tissue (see below).

Replenishment of oxaloacetate and succinate. As mentioned above, the thiotroph seems not to be able to restore its oxaloacetate and succinate pools autonomously, as several TCA cycle enzymes are missing in its genome, and potential anaplerotic routes that could replace the missing enzymes are not encoded (Figures 4a and 5a, see Supplementary Results and Discussion for details). The required intermediates may instead be provided by the host, as suggested by the results of our proteome analysis: The host enzyme phosphoenolpyruvate carboxykinase (PckA, BAGiLS_012326) was abundantly expressed in the *B. azoricus* gill metaproteome and its expression was 3.7 fold higher in the gill as compared to the symbiont-free foot tissue (calculated from host gill and foot OrgNSAF%; Supplementary Table S3). PckA mediates the reversible carboxylation of phosphoenolpyruvate to oxaloacetate (Prichard and Schofield, 1968; Moon *et al.*, 1977; Lee, 2002) and

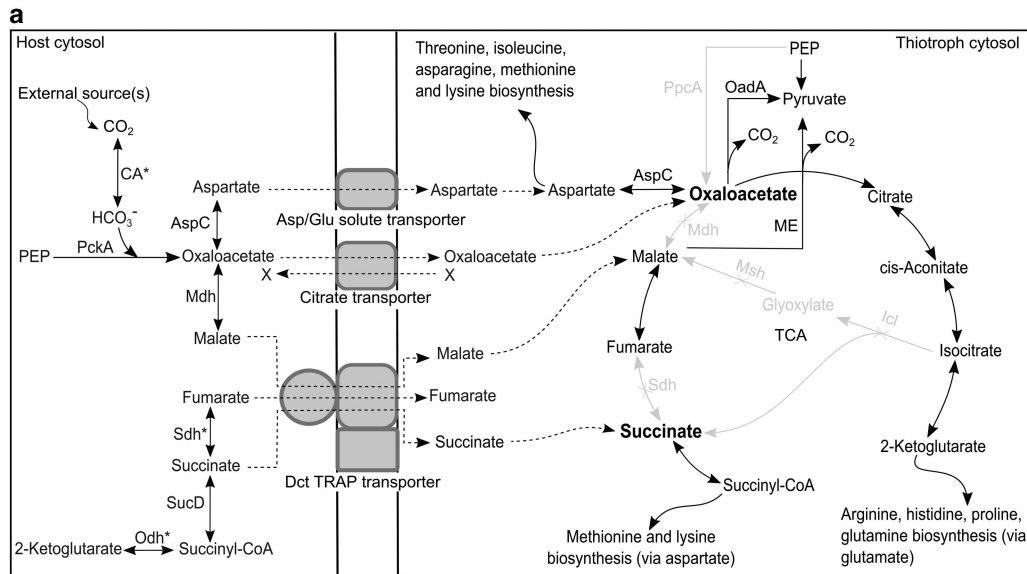
Table 1 Host proteins with putative symbiosis-specific roles

Protein accession number	Protein function	Statistical significance						Expression ratios			
		Group A			Group B			Group A		Group B	
		Gill vs. Foot	Sup vs. Foot	GP vs. Sup	GP vs. Gill	GP vs. Foot	GP vs. Gill	Gill: Foot	Sup: Foot	GP: Sup	GP: Gill
<i>Proteins with putative digestive functions</i>											
BAGiLS_012512	Glycoside hydrolase, family 18, catalytic domain (similar to chitinase)	X						Gill only	Sup only		
BAGiLS_002552	Glycoside hydrolase, family 18, catalytic domain (similar to chitinase)	X						Gill only	Sup only		
BAGiLS_000898	Peptidase M28 (Aminopeptidase Y)	X						26.82	9.38		
BAGiLS_003294	Peptidase, cysteine peptidase active site (Cathepsin protein)	X	X					13.34	23.35		
BAGiLS_021119	Putative beta-glycosidase	X						Gill only	Sup only		
BAGiLS_000621	Sapoin B	X						88.4	114.34		
BAGiLS_005809	Palmitoyl protein thioesterase			X						3.53	3.21
BAGiLS_000071	Peptidase M16, C-terminal			X						15.2	2.39
BAGiLS_000588	Peptidase family M28 (aminopeptidase)				X					1.3	11.92
BAGiLS_000416	Peptidase M16, C-terminal			X						8.14	2.56
BAGiLS_001815	Peptidase M16, C-terminal			X						15.65	5.89
BAGiLS_009112	Peptidase M16, core			X						9.75	1.22
<i>Carbon transport and metabolism</i>											
BAGiLS_001414	CA, carbonic anhydrase, alpha-class, catalytic domain	X	X					10.65	19.21		
BAGiLS_000922	CA, carbonic anhydrase, alpha-class, catalytic domain		X					10.1	15.4		
BAGiLS_005913	Odh, dihydrolipoylysine-residue succinyltransferase component of 2-oxoglutarate dehydrogenase complex			X						24.94	3.16
BAGiLS_010531	Sdh, fumarate reductase/succinate dehydrogenase flavoprotein, C-terminal			X						14.1	1.81
<i>Immune-related functions</i>											
BAGiLS_002519	Sea anemone cytolysin		X								
BAGiLS_009564	Coagulation factor 5/8-type domain protein	X	X								
BAGiLS_003790	C-type lectin										
BAGiLS_008830	sushi domain-containing protein (involved in cell adhesion)	X									
BAGiLS_005314	MD-2-related lipid-recognition domain protein (putative pathogen recognition protein)	X	X							25.36	12.56
BAGiLS_003036	Putative adhesin/invasin	X								41.44	7.21
BAGiLS_019106	Complement C1q protein		X							6.97	13.67

Samples shown in this table were chosen for comparison on the following basis: Group A: to identify putative host proteins that may play a direct role in the symbiosis, gill tissue and supernatant samples (Sup, enriched in host cytosolic proteins from gill tissue) were compared against the symbiont-free foot tissue. Group B: to detect putative host proteins involved in direct interactions with the symbionts (that is, physically linked to the symbionts or the symbiont-surrounding vacuolar membrane), gradient pellet samples (GP, enriched in symbionts) were compared against gill tissue and supernatant samples. Expression ratios were calculated from OrgNSAF% values (averages across all replicates) of the two respective sample types, for example, Gill : Foot, GP : Sup, etc. Proteins detected in only one of the two samples in comparison are indicated by 'Gill only', 'Sup only' and 'GP only'. Significant differences in protein expression levels between two sample types are indicated by 'X' in the Statistical significance columns. A *t*-test with permutation-based false discovery rate (FDR = 5%) was used to test for statistical significance (see methods for details). This table only includes host proteins putatively involved in symbiont digestion, immune-related functions and carbon supply for the thiotrophic symbiont. For additional proteins with putative symbiosis-relevant functions refer to Supplementary Tables S4A and S4B. For protein accession numbers refer to the DeepSeaVent database (<http://transcriptomics.biocant.pt/deepSeaVent/>).

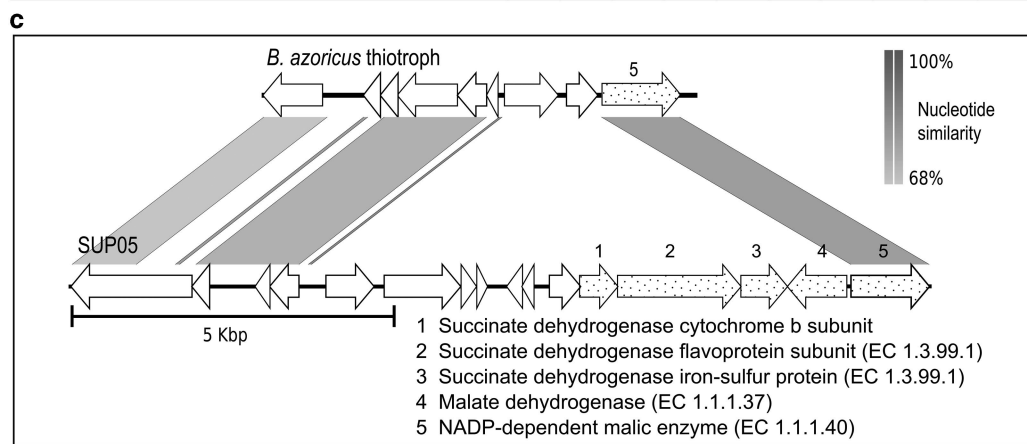
may thus provide oxaloacetate for import into the thiotroph in *B. azoricus* (Figure 5a and b). This would effectively mean that a part of the carbon fixation is

done on the host side. Such an intimate metabolic integration of host and symbiont on the level of central carbon metabolism would provide the host with a



b

Oxaloacetate-replenishing enzyme	Bat*		Bah*		CVo		CRm		CEp		Sup		Arc		Tc	
	Gen	Prot	Prot	Gen	Gen	Gen	Prot									
Malate dehydrogenase, Mdh (EC1.1.1.37)	-	-	+	-	+	+	+	+	+	+	+	-	-	-	-	
PEP carboxylase, PpcA (EC 4.1.1.31)	-	-	-	-	-	-	-	-	-	-	-	-	-	-	+	
PEP carboxykinase, PckA (EC 4.1.1.32)	-	-	+	-	-	-	-	-	-	-	-	-	-	-	-	
Aspartate transaminase, AspC (EC 2.6.1.1)	+	+	+	+	+	+	+	+	+	+	+	+	+	+	+	
Malate:quinone oxidoreductase, Mqo (EC 1.1.5.4)	-	-	-	-	-	-	-	-	-	-	-	-	-	-	+	
Succinate-replenishing enzyme																
Succinate dehydrogenase (EC 1.3.5.1)/Fumarate reductase (EC 1.3.5.4), Sdh/Fmr	-	-	+	-	+	+	+	+	+	+	+	-	-	-	+	
Isocitrate lyase, Icl (EC 4.1.3.1)	-	-	-	-	+	-	-	-	-	-	-	+	-	-		
Malate synthase, Msh (EC 2.3.3.9)	-	-	-	-	-	-	-	-	-	-	-	-	-	-		
2-Oxoglutarate dehydrogenase, Odh (EC 4.1.1.71)	-	-	-	-	-	-	-	-	-	-	-	-	-	-		
Succinate-semialdehyde dehydrogenase (EC 1.2.1.79)	-	-	-	-	-	-	-	-	-	-	-	+	+	+		
Membrane transporters for Oxaloacetate/Succinate																
TRAP C4 acid transport complex (DctQMP)	+	+	-	-	-	+	+	-	-	-	-	-	-	-		
Asp/Glu transporter ABC complex	+	+	-	-	-	-	-	-	-	-	-	-	-	-		
Citrate transporter	+	-	-	+	+	+	-	-	-	-	-	-	-			



direct way to control symbiont metabolism.

Oxaloacetate could furthermore be converted to malate or aspartate before transfer from host to thiotroph (Figure 5a), as indicated by high concentrations of host Mdh (BAGiLS_010003, 0.55% gill OrgNSAF) in the gill metaproteome. The host's aspartate transaminase AspC (CAD42721.2) was also expressed, although at lower abundance (0.012% gill OrgNSAF; Figures 5a and b, Supplementary Table S3). Succinate/succinyl-CoA might be produced or interconverted to fumarate before transfer to the thiotroph by the two host enzymes fumarate reductase/succinate dehydrogenase, Sdh (BAGiLS_010531, Figure 5a), and dihydrolipoyllysine-residue succinyltransferase component of 2-oxoglutarate dehydrogenase, Odh (BAGiLS_005913). Both proteins showed significantly elevated expression levels in the symbiont-enriched gradient pellet as compared to the host-enriched supernatant in our study (Table 1).

Uptake of malate or succinate by the thiotrophic symbiont requires the presence of the TRAP-type C4 dicarboxylate transporter complex DctQMP, whereas aspartate can be imported through the glutamate/aspartate ABC transporter complex, GltIJKL, respectively (Figure 5a). Complete gene sets for both these transporter complexes are encoded in the thiotrophic symbiont's genome. The solute receptor component DctP (BazSymb_scaffold00004_53), a component of the TRAP-type C4 dicarboxylate transporter complex, and the periplasmic binding component GltI (BazSymbA_Acontig00019_5) of the glutamate/aspartate ABC transporter complex were also identified in the thiotroph's proteome (Figure 5b and Supplementary Table S3). Transporters for oxaloacetate are rare in bacteria, but a citrate transporter (BazSymbA_Acontig02368_3), which is encoded in the thiotroph's genome, shows promiscuity towards oxaloacetate as its substrate and may therefore be used for oxaloacetate uptake in the thiotroph (Pudlik and Lolkema, 2011). Oxaloacetate may furthermore also be imported through the above-mentioned TRAP-type C4 dicarboxylate transporter,

which is poorly characterized with respect to its specificity.

Is the thiotroph turning into an obligate symbiont?

The *mdh* and *sdh* genes, which are missing from the thiotroph's genome, are present in a single gene cluster in the symbiont's free-living relative SUP05 (Walsh *et al.*, 2009; Figure 5c). This might indicate a selective loss of these genes during the thiotroph's transition from a free-living to a symbiotic lifestyle, possibly driven by the presence of functional substitutes in the host (as demonstrated in our study). The thiotrophic symbiont may hence even be obligately dependent on the host for its metabolic needs. The fact that no active free-living stage of the thiotrophic *B. azoricus* symbiont has ever been detected in the vent environment might support this speculation. However, as the *mdh* gene (but not the *sdh* gene) is also absent from the recently published genome of the free-living SUP05 member '*Candidatus Thioglobus autotrophica*' (Shah and Morris, 2015), the possibility of an obligate symbiosis in *B. azoricus* remains hypothetical. It might be speculated that a putative free-living stage of the thiotroph – if there is one – may rely on the uptake of oxaloacetate or other small organic molecules from the environment, circumventing the need for the missing TCA cycle enzyme functions.

Adaptations to a symbiotic lifestyle

To identify candidate genes and proteins that are potentially involved in symbiosis-specific functions we pursued two complementary approaches: (i) We compared symbiont genomes and proteomes with those of their free-living relatives. This approach revealed that chaperones and DNA-binding proteins are extraordinarily abundant in both symbionts (see below). It furthermore showed the unexpected presence of genes and proteins involved in CRISPR-Cas and restriction-modification systems in the thiotrophic *B. azoricus* symbiont,

Figure 5 Speculated routes of oxaloacetate and succinate replenishment in the thiotrophic *B. azoricus* symbiont. (a) Incomplete TCA cycle in thiotrophs and possible mechanism of oxaloacetate and succinate replenishment by host enzymes. Enzymes catalyzing reactions shown in grey are not encoded in the *B. azoricus* thiotroph genome. All host enzymes indicated here except AspC are highly abundant in the gill proteome of *B. azoricus* (*these host proteins were detected with significantly elevated expression levels in the symbiont-containing samples, as compared to the symbiont-free foot tissue, see also Table 1). For abundance of the thiotroph's TCA cycle enzymes refer to Figure 4a. A citrate transporter, which might potentially import oxaloacetate (in exchange for an unknown substrate such as pyruvate or acetate indicated in the figure by an X), was not detected in the proteome but is encoded in the thiotroph's genome. The depleted TCA intermediates oxaloacetate and succinate/succinyl-CoA are marked in bold. AspC: aspartate transaminase, Icl: isocitrate lyase, Mdh: malate dehydrogenase, Msh: malate synthase, ME: malic enzyme, OadA: oxaloacetate decarboxylase, Odh: 2-oxoglutarate dehydrogenase, PEP: phosphoenolpyruvate, PckA: PEP carboxykinase, Sdh: succinate dehydrogenase. Note that amino acid biosynthesis from oxaloacetate also involves succinyl-CoA, but that this interconnection of both pathways is not shown in the interest of clarity. (b) Overview of enzymes that can potentially transport or replenish oxaloacetate and succinate in different sulfur-oxidizing Gammaproteobacteria. Presence or absence of the corresponding enzyme gene (Gen) or protein (Prot) is indicated by + and -, respectively. *Data from this study. Bat: *B. azoricus* thiotroph, Bah: *B. azoricus* host (Bettencourt *et al.*, 2010), CVo: *Ca. Vesicomysocius okutanii* (*Calyptogena okutanii* symbiont, Kuwahara *et al.*, 2007), CRm: *Ca. Ruthia magnifica* (*C. magnifica* symbiont, Newton *et al.*, 2007), CEp: *Ca. Endoriftia persephone* (*Riftia pachyptila* symbiont, Markert *et al.*, 2011), Sup: SUP05 (free-living chemoautotroph, Walsh *et al.*, 2009), Arc: ARCTIC96BD-19 (Swan *et al.*, 2011), Tc: *Thiomicrospira crunogena Xcl-2* (Scott *et al.*, 2006). (c) Some TCA cycle enzymes (dotted arrows 1–4) are missing in the *B. azoricus* thiotroph, in contrast to SUP05. See Supplementary Table S2B for genome assemblies included in the gene prediction for this figure.

which may hint at a yet to be determined role of these proteins in host-symbiont interactions (see Supplementary Results and Discussion for details). (ii) We compared protein expression in symbiont-enriched *B. azoricus* samples versus symbiont-free samples, and in symbiont-containing tissue versus symbiont-free tissue to identify host proteins involved in interactions with the symbionts (see Methods for details and Supplementary Table S4 for a comprehensive list of putative symbiosis-relevant proteins identified in our analysis). With this approach we identified a broad repertoire of digestive enzymes, which are likely involved in symbiont digestion (see below). We also detected 23 immune-related host proteins, of which seven had significantly higher expression levels in symbiont-containing samples, and whose exact function in the symbiosis is unclear (see Supplementary Results and Discussion).

High expression of digestive enzymes in gill tissue. In our proteome analysis, we identified 58 host proteins with putative proteolytic and carbohydrate-degrading functions (Supplementary Table S3), of which 12 were significantly more abundant in symbiont-containing samples (whole gills and gradient pellet) compared to symbiont-free (foot tissue) and host-enriched samples (host-enriched supernatant, Table 1). These abundant host enzymes are likely involved in the digestion of the symbionts. In chemoautotrophic invertebrate symbioses, two modes of nutrient transfer from symbiont to host have been proposed: (i) direct digestion of symbionts by the host, and/or (ii) translocation of nutrients from symbiont tissue to the host cells, termed 'milking' (Streams *et al.*, 1997). Although previous observations indicated that symbiont digestion might be the major mode of nutrient transfer in *B. azoricus* (Fisher and Childress, 1992; Streams *et al.*, 1997; Fiala-Médioni *et al.*, 2002), no direct evidence existed so far.

Seven of the host proteins with significantly higher abundances in symbiont-containing samples were putative proteases and peptidases. Among them were lysosomal proteases such as saposin B (BAGiLS_000621) and cathepsin (BAGiLS_003294), which showed >80 fold and ~13 fold higher abundance, respectively, in gills compared to foot samples (Table 1). Lysosomes have been implicated in symbiont digestion in gills of *B. azoricus* (Fiala-Médioni *et al.*, 2002) and other bivalves (Boetius and Felbeck, 1995) and our results further corroborate the idea that lysosomal host proteases may facilitate the degradation of symbiont proteins during symbiont digestion. We furthermore identified two glycosidases (glycoside hydrolases), which were significantly enriched in the gills (Table 1): BAGiLS_012512 was most abundant in the gill membrane fraction, indicating a possible involvement in the hydrolysis of bacterial cell-surface polysaccharides (Davies and Henrissat, 1995; see

Supplementary Table S3). During symbiont digestion, some of the particularly abundant host glycosidases in the gill tissue may also target the methanotrophic symbiont's glycogen reserves (see above).

Abundant chaperones and bacterial nucleoid proteins in B. azoricus symbionts. Our proteome data revealed remarkably high expression levels of molecular chaperones in both symbionts and of histone-like DNA-binding proteins in the thiotrophic symbiont: The chaperones GroEL, GroES, DnaJ and DnaK together constituted 3.02% and 7.16% (gill OrgNSAF) of the total protein abundance in the thiotroph and in the methanotroph, respectively (Velos analysis, see Supplementary Table S3 and Supplementary Results and Discussion). Bacterial nucleoid-associated proteins, such as the histone-like bacterial DNA-binding protein (Hns) and the DNA-binding protein HU beta (HupB), constituted 16.87% (gill OrgNSAF) in the thiotroph, the latter being the most abundant protein of the entire gill metaproteome (Figure 3, Supplementary Table S3). In the thiotroph, GroEL and HupB were even more abundant than the most abundant sulfur oxidation-related protein DsrH and the carbon-fixing RuBisCO. High expression levels of chaperones and DNA-binding proteins have also been observed in other symbionts (Baumann *et al.*, 1996) and in pathogenic bacteria (Neckers and Tatu, 2008), indicating that these proteins might have a symbiosis-specific function in the *B. azoricus* symbionts. As the thiotroph might be evolving into an obligate symbiont (see above), enhanced mutation rates and corresponding increased protein misfolding might be a possible explanation for the observed high chaperone concentrations (see Supplementary Results and Discussion for details).

Conclusion

Our proteogenomic analysis of the deep-sea mussel *B. azoricus* and its two uncultured symbionts provided detailed insights into the molecular mechanisms and strategies that underpin this symbiosis, which is otherwise difficult to access by cultivation-based approaches. The ability of the *B. azoricus* symbionts to use an extensive range of energy sources including sulfide, thiosulfate, methane and hydrogen to fuel chemosynthesis may enable the host to exploit a wide range of environmental conditions. Complementing metabolic pathways between the host and its symbionts point to metabolic interdependence between the individual partners, which may nevertheless enhance the metabolic efficiency of the consortium as a whole. Particularly, the inability of the thiotrophic symbiont to replenish its oxaloacetate and succinate pools and the high abundance of chaperones in their proteome may indicate that this bacterium could be on the

verge of becoming an obligate symbiont. The potential integration of host and symbiont metabolism at the level of TCA cycle intermediates furthermore raises some intriguing questions on how this metabolic interconnection evolved and if it provides a mechanism for the host to exert control on symbiont metabolism. Our study forms a comprehensive basis for future investigations to examine how obligate associations could evolve from facultative symbiotic partnerships.

Conflict of Interest

The authors declare no conflict of interest.

Acknowledgements

Thanks to Captain and Crew of RV Meteor and to C Borowski and D Fink for sampling during the cruise. We appreciate the excellent technical assistance of S Wetzel, J Matulla and S Grund, and are grateful to F Bonn for protein database searches. We thank Antony CP for discussion regarding the methanotroph metabolism. This study was supported by the EU-funded Marie Curie Initial Training Network 'Symbiomics' (project no. 264774). Manuel Kleiner was supported by an NSERC Banting Postdoctoral Fellowship, Lizbeth Sayavedra was supported by a DAAD scholarship, and Jillian M Petersen was supported by the Max Planck Society, and the Vienna Science and Technology Fund (WWTF) through project VRG14-021.

Author contributions

RP performed the FISH analyses, sample preparation for all MS analyses, analysed the proteomes and related genomic data, and wrote the manuscript. MK developed the symbiont enrichment procedure, designed and performed the statistical analysis to identify symbiosis-specific proteins and contributed to the manuscript writing and revision. RP and MK established the protein databases. LS and JP conducted the genome analyses and revised the manuscript. MM, AO and DB performed the MS analyses and AO also conducted database searches. ND supervised and coordinated sampling and genome analysis. TS and StM designed, supervised and coordinated the proteomic analyses, and StM contributed substantially to the manuscript writing and revision.

References

Arp AJ, Childress JJ, Fisher CR. (1984). Metabolic and blood-gas transport characteristics of the hydrothermal vent bivalve *Calyptogena magnifica*. *Physiol Zool* **57**: 648–662.

Arp AJ, Childress JJ, Vetter RD. (1987). The sulphide-binding protein in the blood of the vestimentiferan

tube-worm, *Riftia pachyptila*, is the extracellular haemoglobin. *J Exp Biol* **128**: 139–158.

Baumann P, Baumann L, Clark MA. (1996). Levels of *Buchnera aphidicola* chaperonin GroEL during growth of the aphid *Schizaphis graminum*. *Curr Microbiol* **32**: 279–285.

Beinart R, Gartman A, Sanders J, Luther G, Girguis P. (2015). The uptake and excretion of partially oxidized sulfur expands the repertoire of energy resources metabolized by hydrothermal vent symbioses. *Proc Roy Soc B* **282**: 20142811.

Belkin S, Nelson DC, Jannasch HW. (1986). Symbiotic assimilation of CO₂ in 2 hydrothermal vent animals, the mussel *Bathymodiolus thermophilus* and the tube worm *Riftia pachyptila*. *Biol Bull* **170**: 110–121.

Bettencourt R, Pinheiro M, Egas C, Gomes P, Afonso M, Shank T *et al*. (2010). High-throughput sequencing and analysis of the gill tissue transcriptome from the deep-sea hydrothermal vent mussel *Bathymodiolus azoricus*. *BMC Genomics* **11**: 559.

Boetius A, Felbeck H. (1995). Digestive enzymes in marine invertebrates from hydrothermal vents and other reducing environments. *Mar Biol* **122**: 105–113.

Brune DC. (1995). Sulfur compounds as photosynthetic electron donors. In: Blankenship RE, Madigan MT, Bauer CE (eds), *Anoxygenic Photosynthetic Bacteria*. Kluwer: Dordrecht, The Netherlands, pp 847–870.

Chan SI, Lu YJ, Nagababu P, Maji S, Hung MC, Lee MM *et al*. (2013). Efficient oxidation of methane to methanol by dioxygen mediated by tricopper clusters. *Angew Chem Int Ed* **52**: 3731–3735.

Childress JJ, Fisher CR. (1992). The biology of hydrothermal vent animals – physiology, biochemistry, and autotrophic symbioses. *Oceanogr Mar Biol* **30**: 337–441.

Chistoserdova L, Chen SW, Lapidus A, Lidstrom ME. (2003). Methylo-trophy in *Methylobacterium extorquens* AM1 from a genomic point of view. *J Bacteriol* **185**: 2980–2987.

Colaco A, Bettencourt R, Costa V, Lino S, Lopes H, Martins I *et al*. (2011). LabHorta: a controlled aquarium system for monitoring physiological characteristics of the hydrothermal vent mussel *Bathymodiolus azoricus*. *ICES J Mar Sci* **68**: 349–356.

Company R, Antúnez O, Bebianno MJ, Cajaraville MP, Torreblanca A. (2011). 2-D difference gel electrophoresis approach to assess protein expression profiles in *Bathymodiolus azoricus* from Mid-Atlantic Ridge hydrothermal vents. *J Proteomics* **74**: 2909–2919.

Crowther GJ, Kosaly G, Lidstrom ME. (2008). Formate as the main branch point for methylotrophic metabolism in *Methylobacterium extorquens* AM1. *J Bacteriol* **190**: 5057–5062.

Davies G, Henrissat B. (1995). Structures and mechanisms of glycosyl hydrolases. *Structure* **3**: 853–859.

Dedysh SN, Knief C, Dunfield PF. (2005). *Methylocella* species are facultatively methanotrophic. *J Bacteriol* **187**: 4665–4670.

Distel DL, Lee HK, Cavanaugh CM. (1995). Intracellular coexistence of methano- and thioautotrophic bacteria in a hydrothermal vent mussel. *Proc Natl Acad Sci USA* **92**: 9598–9602.

Doeller JE, Kraus DW, Colacino JM, Wittenberg JB. (1988). Gill hemoglobin may deliver sulfide to bacterial symbionts of *Solemya velum* (Bivalvia, Mollusca). *Biol Bull* **175**: 388–396.

- Duperron S, Bergin C, Zielinski F, Blazejak A, Pernthaler A, McKiness ZP *et al.* (2006). A dual symbiosis shared by two mussel species, *Bathymodiolus azoricus* and *Bathymodiolus puteoserpentis* (Bivalvia: Mytilidae), from hydrothermal vents along the northern Mid-Atlantic Ridge. *Environ Microbiol* **8**: 1441–1447.
- Ellis LL, Burcham JM, Paynter KT, Bishop SH. (1985). Amino acid metabolism in euryhaline bivalves: regulation of glycine accumulation in ribbed mussel gills. *J Exp Zool* **233**: 347–358.
- Fiala-Médioni A, McKiness ZP, Dando P, Boulegue J, Mariotti A, Alayse-Danet AM *et al.* (2002). Ultrastructural, biochemical, and immunological characterization of two populations of the mytilid mussel *Bathymodiolus azoricus* from the Mid-Atlantic Ridge: evidence for a dual symbiosis. *Mar Biol* **141**: 1035–1043.
- Fisher CR, Childress JJ, Oremland RS, Bidigare RR. (1987). The importance of methane and thiosulfate in the metabolism of the bacterial symbionts of two deep-sea mussels. *Mar Biol* **96**: 59–71.
- Fisher CR, Childress JJ, Arp AJ, Brooks JM, Distel D, Favuzzi JA *et al.* (1988). Microhabitat variation in the hydrothermal vent mussel, *Bathymodiolus thermophilus*, at the Rose Garden vent on the Galapagos Rift. *Deep-Sea Res* **35**: 1769–1791.
- Fisher CR, Childress JJ. (1992). Organic-carbon transfer from methanotrophic symbionts to the host hydrocarbon-seep mussel. *Symbiosis* **12**: 221–235.
- Florens L, Carozza MJ, Swanson SK, Fournier M, Coleman MK, Workman JL *et al.* (2006). Analyzing chromatin remodeling complexes using shotgun proteomics and normalized spectral abundance factors. *Methods* **40**: 303–311.
- Gustafson RG, Turner RD, Lutz RA, Vrijenhoek RC. (1998). A new genus and five new species of mussels (Bivalvia, Mytilidae) from deep-sea sulfide/hydrocarbon seeps in the Gulf of Mexico. *Malacologia* **40**: 63–112.
- Harada M, Yoshida T, Kuwahara H, Shimamura S, Takaki Y, Kato C *et al.* (2009). Expression of genes for sulfur oxidation in the intracellular chemoautotrophic symbiont of the deep-sea bivalve *Calyptogena okutanii*. *Extremophiles* **13**: 895–903.
- Hongo Y, Nakamura Y, Shimamura S, Takaki Y, Uematsu K, Toyofuku T *et al.* (2013). Exclusive localization of carbonic anhydrase in bacteriocytes of the deep-sea clam *Calyptogena okutanii* with thioautotrophic symbiotic bacteria. *J Exp Biol* **216**: 4403–4414.
- Kádár E, Bettencourt R, Costa V, Santos RS, Lobo-Da-Cunha A, Dando P. (2005). Experimentally induced endosymbiont loss and re-acquirement in the hydrothermal vent bivalve *Bathymodiolus azoricus*. *J Exp Mar Biol Ecol* **318**: 99–110.
- Kádár E, Davis SA, Lobo-da-Cunha A. (2008). Cytoenzymatic investigation of intracellular digestion in the symbiont-bearing hydrothermal bivalve *Bathymodiolus azoricus*. *Mar Biol* **153**: 995–1004.
- Keltjens JT, Pol A, Reimann J, Op den Camp HJM. (2014). PQQ-dependent methanol dehydrogenases: rare-earth elements make a difference. *Appl Microbiol Biot* **98**: 6163–6183.
- Kleiner M, Petersen JM, Dubilier N. (2012a). Convergent and divergent evolution of metabolism in sulfur-oxidizing symbionts and the role of horizontal gene transfer. *Curr Opin Microbiol* **15**: 621–631.
- Kleiner M, Wentrup C, Lott C, Teeling H, Wetzel S, Young J *et al.* (2012b). Metaproteomics of a gutless marine worm and its symbiotic microbial community reveal unusual pathways for carbon and energy use. *Proc Natl Acad Sci USA* **109**: E1173–E1182.
- Kochevar RE, Childress JJ. (1996). Carbonic anhydrase in deep-sea chemoautotrophic symbioses. *Mar Biol* **125**: 375–383.
- Kuwahara H, Yoshida T, Takaki Y, Shimamura S, Nishi S, Harada M *et al.* (2007). Reduced genome of the thioautotrophic intracellular symbiont in a deep-sea clam, *Calyptogena okutanii*. *Curr Biol* **17**: 881–886.
- Le Pennec M, Donval A, Herry A. (1990). Nutritional strategies of the hydrothermal ecosystem bivalves. *Prog Oceanogr* **24**: 71–80.
- Lee DL. (2002). *The Biology of Nematodes*. Taylor & Francis: London.
- Liu LJ, Stockdreher Y, Koch T, Sun ST, Fan Z, Josten M *et al.* (2014). Thiosulfate transfer mediated by DsrE/TusA homologs from acidothermophilic sulfur-oxidizing archaeon *Metallosphaera cuprina*. *J Biol Chem* **289**: 26949–26959.
- Markert S, Gardebrecht A, Felbeck H, Sievert SM, Klose J, Becher D *et al.* (2011). Status quo in physiological proteomics of the uncultured *Riftia pachyptila* endosymbiont. *Proteomics* **11**: 3106–3117.
- Martins I, Colaço A, Dando PR, Martins I, Desbruyères D, Sarradin P-M *et al.* (2008). Size-dependent variations on the nutritional pathway of *Bathymodiolus azoricus* demonstrated by a C-flux model. *Ecol Model* **217**: 59–71.
- Moon TW, Mustafa T, Hulbert WC, Podesta RB, Mettrick DF. (1977). The phosphoenol-pyruvate branchpoint in adult *Hymenolepis diminuta* (Cestoda): a study of pyruvate kinase and phosphoenol-pyruvate carboxylase. *J Exp Zool A Comp Exp Biol* **200**: 325–336.
- Mueller RS, Deneff VJ, Kalnejais LH, Suttle KB, Thomas BC, Wilmes P *et al.* (2010). Ecological distribution and population physiology defined by proteomics in a natural microbial community. *Mol Syst Biol* **6**: 374.
- Neckers L, Tatu U. (2008). Molecular chaperones in pathogen virulence: emerging new targets for therapy. *Cell Host Microbe* **4**: 519–527.
- Nelson DC, Fisher CR. (1995). Chemoautotrophic and methanotrophic endosymbiotic bacteria at deep-sea vents and seeps. In: Karl DM (ed). *The Microbiology of Deep-sea Hydrothermal Vents*. CRC Press: Boca Raton, FL, pp 125–167.
- Newton ILG, Girguis PR, Cavanaugh CM. (2008). Comparative genomics of vesicomyid clam (Bivalvia: Mollusca) chemosynthetic symbionts. *BMC Genomics* **9**: 585.
- Newton ILG, Woyke T, Auchtung TA, Dilly GF, Dutton RJ, Fisher MC *et al.* (2007). The *Calyptogena magnifica* chemoautotrophic symbiont genome. *Science* **315**: 998–1000.
- Page HM, Fiala-Medioni A, Fisher CR, Childress JJ. (1991). Experimental evidence for filter-feeding by the hydrothermal vent mussel, *Bathymodiolus thermophilus*. *Deep-Sea Res* **38**: 1455–1461.
- Petersen JM, Zielinski FU, Pape T, Seifert R, Moraru C, Amann R *et al.* (2011). Hydrogen is an energy source for hydrothermal vent symbioses. *Nature* **476**: 176–180.
- Powell MA, Somero GN. (1986). Adaptations to sulfide by hydrothermal vent animals – sites and mechanisms of detoxification and metabolism. *Biol Bull* **171**: 274–290.
- Prichard R, Schofield P. (1968). The metabolism of phosphoenolpyruvate and pyruvate in the adult liver fluke *Fasciola hepatica*. *Biochim Biophys Acta* **170**: 63–76.
- Pudlik AM, Lolkema JS. (2011). Mechanism of citrate metabolism by an oxaloacetate decarboxylase-deficient

- mutant of *Lactococcus lactis* IL1403. *J Bacteriol* **193**: 4049–4056.
- Raulfs EC, Macko SA, Van Dover CL. (2004). Tissue and symbiont condition of mussels (*Bathymodiolus thermophilus*) exposed to varying levels of hydrothermal activity. *J Mar Biol Assoc UK* **84**: 229–234.
- Riou V, Colaco A, Bouillon S, Khripounoff A, Dando P, Mangion P *et al.* (2010). Mixotrophy in the deep sea: a dual endosymbiotic hydrothermal mytilid assimilates dissolved and particulate organic matter. *Mar Ecol Prog Ser* **405**: 187–201.
- Sayavedra L, Kleiner M, Ponnudurai RP, Wetzel S, Pelletier E, Barbe V *et al.* (2015). Abundant toxin-related genes in the genomes of beneficial symbionts from deep-sea hydrothermal vent mussels. *eLife* **4**: e07966.
- Scott KM, Sievert SM, Abril FN, Ball LA, Barrett CJ, Blake RA *et al.* (2006). The genome of deep-sea vent chemolithoautotroph *Thiomicrospira crunogena* XCL-2. *PLoS Biol* **4**: e383.
- Shah V, Morris RM. (2015). Genome sequence of ‘*Candidatus Thioglobus autotrophica*’ strain EF1, a chemoautotroph from the SUP05 clade of marine Gammaproteobacteria. *Genome Announc* **3**: e01156–15.
- Streams ME, Fisher CR, Fiala-Médioni A. (1997). Methanotrophic symbiont location and fate of carbon incorporated from methane in a hydrocarbon seep mussel. *Mar Biol* **129**: 465–476.
- Swan BK, Martinez-Garcia M, Preston CM, Sczyrba A, Woyke T, Lamy D *et al.* (2011). Potential for chemolithoautotrophy among ubiquitous bacteria lineages in the dark ocean. *Science* **333**: 1296–1300.
- Van Dover CL. (2000). *The Ecology of Deep-sea Hydrothermal Vents*. Princeton University Press: New Jersey.
- Vizcaíno JA, Csordas A, del-Toro N, Dianes JA, Griss J, Lavidas I *et al.* (2016). 2016 update of the PRIDE database and its related tools. *Nucleic Acids Res* **44**: D447–D456.
- von Cosel R, Comtet T, Krylova E. (1999). *Bathymodiolus* (Bivalvia: Mytilidae) from the hydrothermal vents on the Azores Triple Junction and the Logatchev hydrothermal field, Mid-Atlantic Ridge. *Veliger* **42**: 218–248.
- Walsh DA, Zaikova E, Howes CG, Song YC, Wright JJ, Tringe SG *et al.* (2009). Metagenome of a versatile chemolithoautotroph from expanding oceanic dead zones. *Science* **326**: 578–582.
- Wood AP, Aurikko JP, Kelly DP. (2004). A challenge for 21st century molecular biology and biochemistry: what are the causes of obligate autotrophy and methanotrophy? *FEMS Microbiol Rev* **28**: 335–352.
- Zhao S-J, Hanson RS. (1984). Variants of the obligate methanotroph isolate 761M capable of growth on glucose in the absence of methane. *Appl Environ Microbiol* **48**: 807–812.



This work is licensed under a Creative Commons Attribution-NonCommercial-ShareAlike 4.0 International License. The images or other third party material in this article are included in the article's Creative Commons license, unless indicated otherwise in the credit line; if the material is not included under the Creative Commons license, users will need to obtain permission from the license holder to reproduce the material. To view a copy of this license, visit <http://creativecommons.org/licenses/by-nc-sa/4.0/>

Supplementary Information accompanies this paper on The ISME Journal website (<http://www.nature.com/ismej>)